# A clinically applicable approach for higher spatiotemporal resolution thermometry mapping

Feng Huang[1], Max Köhler[2], Jukka Tanttu[2], Roel Deckers[3], Wei Lin[1], and George Randy Duensing[1]
[1]Invivo Corporation, Gainesville, FL, United States, [2]Philips Healthcare, Vantaa, Finland, [3]University Medical Center Utrecht, Image Sciences Institute, Utrecht, Netherlands

## Introduction

MRI is being increasingly used for planning, but also for guidance of thermal therapies including HIFU (High-Intensity Focused Ultrasound) by means of MR thermometry. In order to ensure a safe ablation procedure, high spatiotemporal resolution temperature mapping is necessary. Since the thermometry is commonly performed by acquiring phase images and measuring the change in the proton resonance frequency (PRF), there is therefore a need for faster phase imaging without compromising SNR (Signal-to-Noise Ratio) that can alternatively also be used for increasing the spatial coverage. Furthermore, the reconstruction time has to be fast enough to enable real-time monitoring of the temperature rise that is needed for a safe therapy procedure. In this work, a variable density acquisition scheme and spatially adaptive convolution in *k*/*k*-*t* space reconstruction scheme are proposed for this purpose. Without using any assumption [1] or model [2] of the temperature, the proposed method takes advantages of redundant information among multi-channels and time frames to achieve accurate reconstruction at high acceleration factors. Using a 5-channel coil, net reduction factor 4 can be achieved with an error of only -0.3±0.8°C. Moreover, the reconstruction speed is suitable for real time applications.

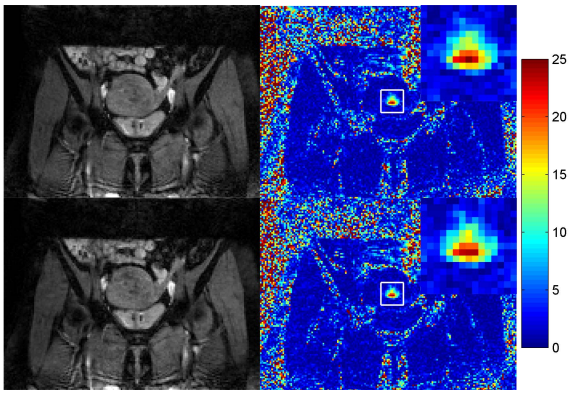


**Figure 1**. Magnitude and temperature map of the time frame with maximum temperature rise for R = 1 (first row) and R = 4 (second row). The right upper corners show the zoomed in regions in the white boxes. Data set 2 was used.

## Methods

***Acquisition Trajectory:*** A variable density acquisition trajectory is used. The center *k*-space uses a low reduction factor to ensure the accuracy of the low frequency information. In the current implementation, the central 40 lines use a reduction factor of 2. The outer *k*-space uses higher acceleration factor, such as 7. The outer *k*-space uses a time interleaved trajectory, which is conventionally adopted in *k*-*t* methods [3, 4]. An optimized interleave scheme [5] is also used.

***Reconstruction Scheme:*** There are two steps for the center and outer *k*-space respectively. GRAPPA [6] is used for reconstruction of the center *k*-space. The calibration signal for GRAPPA is from the reference image that is acquired before the start of the HIFU sonication [7]. The reconstruction result of GRAPPA is used for kernel calibration in the next step for outer *k*-space. *k*-*t* GRAPPA [4] is used for reconstruction of the outer *k*-space. Only the information from the previous time frames is used in *k*-*t* GRAPPA for this real-time application. As discussed in the original *k*-*t* GRAPPA paper, it is important to reduce image support before convolution in *k*-*t* space. For the data used for the PRF thermometry, all partially acquired data requires the reference data to be subtracted at the acquisition location to reduce image support. After the convolution in *k*-*t* space, the subtracted data will be returned to the images.

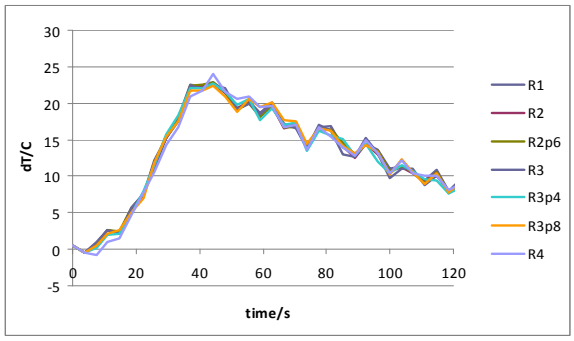


**Figure 2**. $T_{peak}$ as a function of time of data set 2.

***Experimental setup***: MR thermometry data was acquired during 5 clinical uterine fibroid HIFU sonications in two patients. The sonications were all feedback sonications performed at 1.2 MHz using the Sonalleve V2 MR-HIFU platform with its 5-ch coil integrated into a 1.5 T Philips Achieva MR scanner. Other sonication parameters are given in Tab. 2. The sequence used for thermometry was gradient-echo EPI images of a clinical MR-HIFU uterine fibroid ablation were acquired with parameters (5 coronal slices, 1 sagittal slice, TR = 41ms, TE = 19ms, resolution = 2.5×2.5×7mm$^3$, FOV 400×310, flip angle 20°, EPI factor = 11, temp. res.= 3.7s). An axial REST slab was also placed in the upper abdomen and used to suppress artifacts arising from the heavy breathing of these patients. The fully acquired data was artificially downsampled at net reduction factors 2, 2.6, 3, 3.4, 3.8, and 4 using the proposed trajectories. The calculated temperature using partially acquired data was compared with that using fully acquired data. $T_{peak}$ is the highest temperature in the heated region.

## Results and Discussion

Figs. 1-2 and Tables 1-2 show the results and comparison. The coronal slice centered on the HIFU heating was used in the Figures and Tables. Celsius was used in all Figures and Tables. It can be seen that the results with accelerated data are close to those at R = 1. Even the results at R =4, the largest average error of 5 data sets was 0.3°C. Moreover, the accuracy was preserved when the temperature was increased by over 25°C in about 40 seconds with the spatial distribution of the heated area remaining unaffected (Fig. 1). The insensitivity to motion is another advantage of the proposed method. Even though clear bowel movement can be observed, the reconstruction can still be accurate. For the data set with matrix size 160×120×5 for each slice, the total processing time with un-optimized Matlab code was about 2 seconds. Hence, the processing time can potentially meet the requirement of real time applications. One potential problem of the proposed method is the temperature tends to be underestimated during the heating period if the net reduction factor is very high. In conclusion, variable density acquisition trajectory and convolution in *k*-*t* space reconstruction is robust to motion and can significantly improve the spatiotemporal resolution of real-time temperature mapping of clinical HIFU ablations without compromising the accuracy of the detected temperature rise. The improved acquisition speed can also be used for improving the spatial coverage of the thermometry potentially further improving the safety of the HIFU therapy.

**Table 1. Average and standard deviation of the temperature difference (°C) of the curves in Fig. 2**

| | R2 | R2.6 | R3 | R3.4 | R3.8 | R4 |
|---|---|---|---|---|---|---|
| ave | -0.19 | -0.13 | -0.22 | -0.24 | -0.12 | -0.32 |
| std | 0.20 | 0.28 | 0.48 | 0.63 | 0.49 | 0.84 |

**Table 2. Temperature errors (°C) of all 5 data sets at R = 4**

| Data set | 1 | 2 | 3 | 4 | 5 |
|---|---|---|---|---|---|
| $T_{peak}$ | 25.4 | 24.9 | 22.3 | 29.5 | 29.1 |
| ave | 0.3 | -0.3 | -0.08 | -0.11 | -0.01 |
| std | 0.8 | 0.8 | 0.6 | 0.6 | 0.8 |
| Cell size (mm) | 8 | 8 | 16 | 16 | 12 |
| Power (W) | 150 | 130 | 120 | 130 | 130 |
| Duration (s) | 36 | 36 | 46 | 68 | 42 |

## References :

[1] Todd, N., et. al. MRM 2009;62:406-419
[2] Todd, N., et. al. MRM 2010; 63:1269-1279.
[3] Tsao, J., et. al. MRM, 2003;50(5):1031-1042
[4] Huang, F., et. al. MRM 2005; 54(5):1172-1184
[5] Tsao, J., et. al. MRM, 2005;53:1372-1382.
[6] Griswold, M. A., et. al. MRM, 2002; 47: 1202-1210
[7] De Poorter J. MRM 1995;34(3):359-367